Biomedicine & Pharmacotherapy 205 (2026) 120050



Contents lists available at ScienceDirect

Biomedicine & Pharmacotherapy

journal homepage: www.elsevier.com/locate/biopha

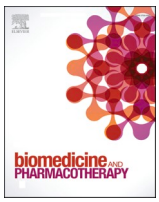

Nicotinamide phosphoribosyltransferase (NAMPT) inhibitors selectively induce cell death in human glioblastoma stem cells: Perspectives for preventing glioblastoma recurrence

Alessia Buccellini [a], Paolo Cabras [b], Ubaldina Galli [c], Daniela Buonocore [d], Francesco Raimondi [e], Cristina Lanni [a], Marco Peviani [d], Cristina Travelli [a], Mayra Paolillo [f,*]

[a] Universita degli Studi di Pavia, Dipartimento di Scienze del Farmaco, Italy
[b] Universita di Pavia, Dipartimento di Biologia e Biotecnologie L Spallanzani, Italy
[c] Università degli Studi del Piemonte Orientale Amedeo Avogadro,Dipartimento di Scienze del Farmaco, Italy
[d] Università di Pavia, Dipartimento di Biologia e Biotecnologie L Spallanzani, Italy
[e] Scuola Normale Superiore, Italy
[f] Universita degli Studi di Pavia, Dipartimento di Scienze del Farmaco, Italy

ARTICLE INFO

Keywords:
Glioblastoma stem cell eradication
NAD salvage pathway dependency
NAPRT loss
Targeted post-operative therapy
Relapse prevention

ABSTRACT

Glioblastoma recurrence, largely driven by chemo- and radiotherapy-resistant glioma stem cells, remains a major clinical obstacle. Although nicotinamide phosphoribosyltransferase is key to cancer metabolism, past clinical trials with systemic inhibitors failed due to severe toxicity and limited efficacy against the bulk tumor mass. This study investigates whether nicotinamide phosphoribosyltransferase targeting can be repurposed, shifting the focus from reducing primary tumor size to selectively eliminating patient-derived glioblastoma stem cells to prevent relapses.

Methods: We assessed nicotinamide phosphoribosyltransferase expression and metabolic dependence in patient-derived glioblastoma stem cells, standard glioblastoma cell lines, and non-malignant human cells (astrocytes, endothelial cells, and differentiated neurons). Cytotoxicity, apoptosis, and therapeutic selectivity of small-molecule inhibitors were analyzed alongside enzyme-silencing experiments.

Results: Patient-derived glioblastoma stem cells showed high nicotinamide phosphoribosyltransferase levels together with negligible nicotinate phosphoribosyltransferase expression, making them strictly dependent on the salvage pathway. Synthetic nicotinamide phosphoribosyltransferase inhibitors induced apoptosis in glioblastoma stem cells at nanomolar or picomolar concentrations, whereas non-malignant neural and vascular cells tolerated doses up to the micromolar range. Standard glioblastoma cell lines were considerably less sensitive, failing to reflect stem cell responses. Finally, genetic silencing of nicotinamide phosphoribosyltransferase mimicked inhibitor-induced toxicity, confirming target-specific action.

Conclusion: These results reveal a clear therapeutic window for nicotinamide phosphoribosyltransferase inhibitors. Instead of broad systemic use against primary tumors, these agents could serve as targeted post-operative tools to eradicate residual stem cells and reduce the risk of glioblastoma recurrence.

1. Introduction

Glioblastoma multiforme (GBM) is classified as a grade IV glioma and is recognized as the most aggressive and malignant form of primary brain tumor [1]. GBM can be either primary (de novo) or secondary, when it is arising from the progression of a low-grade glioma. GBM represents the vast majority of cases (94.7%), accounting for approximately 57% of all gliomas and 48.6% of all malignant central nervous system (CNS) tumors [2,3]. GBM is notorious for its poor prognosis and, despite the efforts made so far to find an effective therapy and identify new molecular targets, patients generally have a poor outlook, with long-term survival often limited to a few months or years after diagnosis.

* Corresponding author.
E-mail address: mayra.paolillo@unipv.it (M. Paolillo).

https://doi.org/10.1016/j.biopha.2026.120050
Received 17 September 2026; Received in revised form 30 October 2026; Accepted 6 November 2026
Available online 19 November 2026
0753-3322/© 2026 The Author(s). Published by Elsevier Masson SAS. This is an open access article under the CC BY license (http://creativecommons.org/licenses/by/4.0/).

A number of genetic alterations have been identified in GBM, including mutations in EGFR, PTEN, NF1, and TP53 genes, as well as IDH1/2 and TERT promoter mutations, but no one is considered a potential drug target, at the moment.

Cancer stem cells (CSCs), specifically glioma stem cells (GSCs), play a crucial role in GBM initiation, maintenance, and recurrence. These cells have the ability to self-renew, drive tumor heterogeneity and contribute to the treatment resistance and tumor relapses. GSCs share many features with neural stem cells, including the expression of markers like CD133, CD44, SOX2, and Nestin1 [4]. These characteristics, together with their high capacity for infiltrating healthy tissue, suggest that GSCs are primarily responsible for recurrence; thus, they represent an excellent, albeit challenging, therapeutic target.

Nicotinamide phosphoribosyltransferase (NAMPT) is a pivotal enzyme that governs the synthesis of nicotinamide adenine dinucleotide (NAD+), thereby critically influencing cellular metabolic regulation, reprogramming, apoptosis, and senescence [5,6]. This enzyme, initially characterized for its enzymatic activity in 1957, possesses a molecular weight of approximately 55 kDa and comprises 491 amino acids, existing as a dimeric type II phosphoribosyltransferase [7].

Nicotinic acid phosphoribosyltransferase (NAPRT) is the key rate-limiting enzyme regulating the Preiss-Handler pathway, an alternative biochemical route that allows cells to synthesize NAD + from nicotinic acid (NA). While most healthy tissues possess a redundant system in which both the NAMPT-mediated salvage pathway and the NAPRT pathway coexist, a very high percentage of GBM displays epigenetic silencing due to promoter hypermethylation or homozygous deletion of the NAPRT gene. This specific genetic alteration deprives tumor cells of the Preiss-Handler pathway, thus making them entirely dependent on the NAMPT/NAD + axis for their survival [8,9]. In GSCs this axis is also essential to maintain the stemness features [10–12].

However, NAMPT significance extends beyond its enzymatic activity, implicating it as a central regulator in cell metabolism and a key player in the initiation and progression of diverse malignancies, including breast cancer, prostate cancer, melanoma, and glioblastoma [5]. Within the intricate network of cellular metabolism, in fact, NAMPT plays a critical role in sustaining a multitude of biological processes, including DNA repair, cell cycle regulation, and chromatin dynamics.

Despite its role in cancer biology, highlighted by recent papers [13,14], the intricate details of its involvement in glioblastoma pathogenesis and progression remain an area of active investigation.

Indeed, although NAMPT has been identified as a gene signature in high-grade gliomas [12], therapeutic attempts to target NAMPT did not lead to successful trials, often due to inhibitor-linked cell toxicity [13]. The main reason for therapeutic failure in GBM is disease recurrence, which is driven by the high infiltrative capacity of GSCs. Current therapies primarily target the differentiated bulk of the tumor, thereby leaving GSCs viable and effectively selecting for a resistant cell population that predisposes to relapse. For this reason, in this study we decided to investigate the effect of NAMPT inhibitors on GSCs, comparing them with other non-tumor cells, with the aim of targeting not the tumor mass as a whole, but specifically the cell population that survives chemo- and radiotherapy and drives disease recurrence.

We evaluated NAMPT expression and contribution to GSC survival in different human glioblastoma stem cells, a GBM cell line and normal human astrocytes, endothelial cells and differentiated neuron-like SH-SY5Y cells with the aim of selectively target GSCs by using newly synthesized NAMPT inhibitors.

We found that the expression of NAMPT, both at the mRNA and protein level, is higher in GSCs compared to glioma cell and other non-tumor cells. Treatment with NAMPT inhibitors drastically reduced the cell viability of GSCs even at extremely low concentrations (1–5 nM), while no effects were observed on astrocytes and other cell lines. Silencing NAMPT following siRNA treatment mimicked the effect of the inhibitors, thus highlighting NAMPT as a specific target of the inhibitors and confirming its key role in GSC survival. This work also demonstrates that differentiated GBM cell lines do not represent a good experimental model for the study of NAMPT inhibitors due to their low sensitivity; moreover, the high sensitivity of GSCs to the inhibitors and the high selectivity of these molecules toward GSCs highlights these small molecules as pharmacological tools suitable for preventing relapses rather than targeting the tumor mass as a whole—how they have been conceived and utilized until today. Indeed, relapses are primarily driven by the infiltrative capacity of GSCs, which are resistant to conventional chemo- and radiotherapy. Therefore, the potent cytotoxic of NAMPT inhibitors against GSCs positions them as promising drug candidates to target a tumor cell population which has remained largely untouched by current standard therapies.

2. Materials and methods

2.1. Cell culture

U251 human glioblastoma cell lines were purchased from the ECACC collection (Merck Life Science, Milan, Italy) and maintained in culture under standard growth conditions (DMEM/F12 supplemented with 5% (v/v) fetal bovine serum, 1% (v/v) penicillin-streptomycin, and 1% (v/v) L-glutamine). All the reagents for cell culture were purchased from Merck KGaA, Darmstadt, Germany.

Normal human astrocytes (NHA) were obtained from ScienCell Research Laboratories (Carlsbad, CA, USA) and grown in DMEM plus 5% (v/v) FBS. Forty-eight hours before the experiments, the media for NHA and U251 cells were replaced with DMEM/F12 supplemented with 1% (v/v) fetal bovine serum.

GSC1, GSC2, GSC3 were isolated from patients at the Neurosurgery Department of the Institute for Research, Hospitalization and Care-University Hospital (IRCCS-AOU) San Martino-Cancer Research Institute (IST) (Genoa, Italy), grown and characterized as previously described (DMEM/F12 and neurobasal medium mixed 1:1 ratio and supplemented with 1% GlutaMAX™, 1% penicillin-streptomycin, 1% B-27 and N2 supplements, 10 ng/mL bFGF and 20 ng/mL EGF) [15]. Prior to initiating the experimental procedures, GSCs were tested to verify the expression of stemness and EMT markers (table S1 and fig S1 in supplementary data).

Human Umbilical Vein Endothelial Cells (HUVECs) from PromoCell (Heidelberg, Germany) were cultured in Endothelial Cell Growth Medium (Cell Applications, Inc., San Diego, CA, USA).

Human neuroblastoma-derived, neuron-like SH-SY5Y cells (ATCC® CRL-2266™), exhibiting an epithelial morphology and originally isolated from the bone marrow of a 4-year-old female, were cultured as mixed, suspension and adherent monolayer in DMEM/F12 (1:1) (1 ×) medium (Gibco, Cat. No. 11320–033, Lot No. 2715697). The medium was supplemented with 10% non-heat-inactivated fetal bovine serum (FBS) and a 1% penicillin/streptomycin antibiotic mixture. Cells (starting from passage number p37) were maintained in T75 flasks at 37 °C in a humidified atmosphere containing 5% CO_2.

SH-SY5Y cells can be differentiated to a more mature neuron-like phenotype that was characterized by neuronal markers [16]. Specifically, the differentiation protocol for SH-SY5Y cells developed by Shirley et al. was followed [17], with in-house modifications adapted to enable toxicity/cell viability and other assays in 96-well plates (not published) (Fig. S2).

2.2. Drugs

FK866 was commercially available (AdipoGen Life Sciences). MV87 and MV78, two triazole-based NAMPT inhibitors, were synthetized as described previously [18] by the medicinal chemistry laboratory at the University of Novara. The Inhibitors were dissolved in DMSO at 10 mM, and kept at −20 °C.

2.3. Real-time RT-qPCR

To assess NAMPT and NAPRT expression in NHA, U251, GSC1, GSC2, and GSC3, NAMPT and NAPRT mRNA was evaluated by quantitative real-time RT-PCR. Total RNA was extracted from cells using Rneasy Mini Kit (QIAGEN, Hilden, Germany), following the manufacturer instructions and RNA quantification was performed by NanoReady Touch FC-3100 (Hangzhou LifeReal Biotechnology, Hangzhou, China). 0,5 μg total RNA was reverse transcribed using QuantiTect® Reverse Transcription Kit (QIAGEN, Hilden, Germany) following the manufacturer's instructions. qPCR was performed using QuantiTect® Sybr Green PCR Kit (QIAGEN, Hilden, Germany) and CFX Opus 96 (Bio-Rad, Hercules, CA, USA). The following primers were used: NAMPT (Gene ID: 10135; NM_005746.3), F: AGGGTTACAAGTTGCTGCCACC; R: CTCCACCAGAACCGAAGGCAAT. NAPRT (Gene ID: 93100), F: GCCCACTCCTTTGTCACTTC; R: AAGTAGAGGCACACACGCTT; GAPDH (Gene ID: 2597; NM_002046.7) was used as a housekeeping gene, F: CAACTGTGAGGAGGGGAGATT; R: CAGCAAGAGCACAAGAGGAAG.

We also compared the expression of stemness and EMT markers in GSCs and NHAs, as a control for our experimental model. Related methods and results are reported in the supplementary material. Experiments were performed on three different cell preparations; each run was analyzed in duplicate and transcripts quantification was performed by the $2^{(-\Delta\Delta CT)}$ method [19].

2.4. Western blot analysis

Cells were plated in 60-mm dishes and lysed as previously described 2. Protein quantification was performed by Bradford protein assay (Merck KGaA), and 40 μg of proteins were separated by SDS-PAGE on 10%, 12%, or 15% polyacrylamide gels, and transferred onto nitrocellulose membranes using the Trans-Blot® Turbo™ Transfer System (Bio-Rad, Hercules, CA, USA). The membranes were first blocked for 1 h in Tris buffered saline solution (TBST composition: Tris 10 mM, NaCl 150 mM, 0.1% v/v Tween 20) plus 5% low fat dry milk (TBSTM) and then rinsed three times in TBST. After blocking, the membranes were incubated with primary antibodies after appropriate dilution in TBSTM overnight at 4 °C under gentle agitation. The membranes were then rinsed three times in TBST and incubated for 1 h at room temperature (RT) with an anti-mouse secondary antibody (1:5000 dilution) or an anti-rabbit secondary antibody (1:10000 dilution), both diluted in TBSTM. After another three washes in TBST, immunoblot images were acquired using ChemiDoc MP Imaging System (Bio-Rad, Hercules, CA, USA) and the optical density of the bands was determined using ImageJ software.

The following primary antibodies were used: mouse anti-NAMPT (Cat. No. AG-20A-0034-C050, AdipoGen Life Sciences, San Diego, CA, USA), diluted 1:2000; rabbit anti-β-actin (Cat. No. 31–1013–00, RevMab Biosciences, Burlingame, CA, USA), 1:1000; rabbit anti-caspase-8 p18 (Cat. No. sc-7890, Santa Cruz Biotechnology, Santa Cruz, CA, USA), 1:500; rabbit anti-LC3 (Cat. No. 2775, Cell Signaling Technology, Danvers, MA, USA) 1:1000; and rabbit anti-Beclin-1 (Cat. No. sc-11427, Santa Cruz Biotechnology), 1:1000. β-Actin was used as the loading control. All experiments were performed at least in duplicate, except for NAMPT protein expression analysis, which was performed in quadruplicate.

2.5. Immunocytochemical analysis

Glioblastoma stem cells and human primary astrocytes were seeded at a density of 5×10^4 cells per well in a 24-well plate previously coated with poly-D-lysine. The coating was performed using 50 μg/mL poly-D-lysine (MedChemExpress, Cat. No. HY-139201A) diluted in sterile H_2O and incubated for 4 h at 37 °C in 5% CO_2. After 24 h, half of the culture medium was replaced with an equal volume of 4% paraformaldehyde (PFA) to fix the cells for 20 min at room temperature (RT). Fixed cells were then washed three times with PBS 1 × containing Ca^{2+} and Mg^{2+}. Cells were permeabilized and blocked by incubating them for 1 h at RT with blocking buffer composed of 3% bovine serum albumin (BSA) and 0.1% Triton X-100 in PBS. Cells were then incubated with the primary antibody mouse anti-NAMPT (dilution 1:500) for 1 h at RT, followed by overnight incubation at 4 °C. The following day, cells were washed three times with PBS 1 × and incubated with the secondary antibody Donkey anti-Mouse Alexa Fluor 568 (Invitrogen Cat. No. a10037; dilution 1:500) for 1 h at RT in the dark. After washing, nuclei were counterstained with DAPI (SERVA, Cat. No. 18860.01, dilution 1:10,000) for 10 min at RT. Immunofluorescence images were acquired using a Leica SP5 confocal microscope at 40 × magnification. To assess non-specific binding of the secondary antibody, a negative control was performed by omitting the primary antibody during the staining procedure.

2.6. ELISA

To assess whether NAMPT protein was released (eNAMPT) by NHA, GSC1, GSC2, and GSC3, eNAMPT/Visfatin was evaluated using a commercial Human Visfatin ELISA Kit (Thermo Fisher Scientific) according to the manufacturer's instructions. Cells were grown for 5 days on 12-well plates at a density of 5×10^4 cells/well; afterwards, the medium was collected and centrifuged at 12,000 rpm for 10 min at 4 °C. Cell-free supernatants were stored at −80 °C until measurement. Results are expressed as ng/mL and each experiment was repeated three times.

2.7. Cell viability assays

Cell viability assays were performed after 48 h treatments with inhibitors at 1 nM, 5 nM, 10 nM, 100 nM, 1 μM, concentrations using the MTS assay (CellTiter 96 AQueous One Solution Cell Proliferation assay; Promega Corporation, Madison, WI, USA). NHA and U251 cells were seeded at a density of 3.5×10^3 cells/well in 96-well plates, kept in culture for 48 h in 1% FBS medium and then treated as indicated for 48 h. GSCs were seeded at a density of 3.5×10^3 cells/well in 96-well plates, kept in culture for 48 h in their growth medium and then treated as indicated for 48 h. HUVECs were also seeded at a density of 3.5×10^3 cells/well in 96-well plates. Differentiated neuron-like SH-SY5Y cells were seeded into 96-well plates at density of 2.2×10^4 cells/well. Cell viability was assessed after 21 days of differentiation, and following 48 h of treatment as described.

After treatments, MTS solution was added in each well and after 1.5 h of incubation at 37°C the plates were read at 490 nm using a Synergy™ HT Microplate Reader (BioTek, Swindon, UK). All experiments were performed at least three times in quadruplicate, and data are expressed as percent of living cells of the experimental wells compared to the control wells.

2.8. NADH assay

Total NADH/NADPH content in lysates from NHA, GSC1, GSC2, GSC3, and U251 cells was determined using the NADH and NADPH Assay Kit (ab186031, Abcam, Cambridge, UK), according to the manufacturer's instructions. Cells were cultured in 60 mm dishes and treated with 5 nM of MV78 for 48 h. Absorbance was measured at 460 nm using a Synergy™ HT Microplate Reader (BioTek). Results were normalized to total protein content determined by the Bradford assay (Merck KGaA). The experiment was performed three times in triplicate.

2.9. FACS analysis

NHA and GSC 1 were plated in 60 mm dishes at a density of 150,000 cells per dish and treated with 5 nM FK866 or MV78 for 48 h. After gentle scraping, cells were washed once with PBS and once with binding buffer and stained with Annexin IV and propidium iodide (PI) using the Annexin V Apoptosis Detection Kit FITC (Cat. No. 88–8005–72, Thermo

Fisher Scientific) according to the manufacturer's instructions. 10,000 cells were analyzed for each sample using a BD FACS Lyric™ flow cytometer (BD Biosciences, Franklin Lakes, NJ, USA). All experiments were repeated at least twice.

2.10. Senescence assay

Cellular senescence was assessed using the Mammalian β-Galactosidase Assay Kit (Thermo Fisher Scientific). Cells were plated in 60 mm dishes and, after reaching the desired confluence, treated with 5 nM FK866, MV78, or MV87 for 48 h. Cells were then collected, lysed, and centrifuged at 10,000 rpm for 8 min at 4 °C. The supernatants were collected, and protein quantification was determined using the Bradford protein assay (Merck KGaA). Equal volumes of sample and substrate solution were added to a 96-well plate. After incubation for 30 min at 37 °C, absorbance was measured at 405 nm using a Synergy™ HT Microplate Reader (BioTek). β-Galactosidase activity was normalized to total protein content.

2.11. Silencing of NAMPT in glioma stem cells

NAMPT silencing was achieved using Accell siRNA technology (Dharmacon, Horizon Discovery), a delivery system optimized for difficult-to-transfect cells such as glioblastoma stem cells (GSCs). This non-viral, transfection reagent-free approach avoids the cytotoxicity commonly associated with traditional transfection methods. The procedure was carried out according to the manufacturer's standard protocol. GSCs 1 were seeded at a density of 5×10^4 cells per well in a 24-well plate previously coated with poly-D-lysine (50 μg/mL) and incubated overnight at 37 °C with 5% CO_2. Accell siRNA targeting human NAMPT (Cat. No. A-004581–13–0010) was prepared by diluting a 100 μM stock 1:100 in Accell Delivery Media (Cat. No. B-005000), resulting in a final siRNA concentration of 1 μM in a total volume of 500 μL per well. The siRNA-containing medium was freshly prepared and applied immediately after dilution. Cells were incubated with the Accell siRNA at 37 °C in 5% CO_2 for 72 or 96 h, depending on the experimental endpoint. To monitor intracellular uptake of the siRNA, a Cy3-labeled non-targeting siRNA (Accell Control siRNA Kit Red, Cat. No. K-005000-R1–0Y) was used. Fluorescence images were acquired daily using both brightfield and RFP channels. For validation of knockdown specificity and efficiency, Accell GAPD Control siRNA (positive control; Cat. No. D-001930–0Y) and Accell Cyclophilin B Control siRNA (negative control; Cat. No. D-001920–0Y) were included. After 72 h, cells were harvested, and a 3 × 105 cells pellet was collected for each experimental condition and resuspended using Buffer RLT supplemented with 1% β-mercaptoethanol, as provided in the RNeasy Plus Micro Kit (Qiagen, Cat. No. 74034). After resuspension, cell lysate was immediately frozen at −80 °C. mRNA knockdown was quantified by RT-qPCR, while protein knockdown was assessed after prolonged incubation (≥96 h) via Western Blot.

2.12. Kaplan-Meier survival curves

Kaplan-Meier survival curves stratifying patients based on NAMPT expression in TCGA, were generated for both glioblastoma multiforme (GBM) and lower-grade glioma (LGG) using the webserver https://tcga-survival.com/ (https://github.com/joan-smith/comprehensive-tcga-survival [PMID: 35354049]).

2.13. Statistical analysis

Statistical analyses were performed using GraphPad Prism version 11 (GraphPad Software, San Diego, CA, USA). Statistical differences were determined by analysis of variance (ANOVA) or Student's *t*-test and, when significant, followed by an appropriate post hoc test, as indicated in the figure legends of the Results section. Differences were considered statistically significant at $p < 0.05$. Data are presented as the mean ± standard deviation (SD) of at least three independent experiments.

3. Results

3.1. NAMPT is differently expressed in NHA, GSCs, and U251 cell line

Initially, we evaluated the relationship between NAMPT expression and the survival of patients affected by GBM and low-grade gliomas (LGG), using The Cancer Genome Atlas (TCGA), a landmark cancer genomics program that sequenced and molecularly characterized over 11,000 cases of primary cancer samples [PMID: 35354049]. Kaplan-Meier survival analyses were performed for TCGA cohorts (GBM and LGG), stratified by NAMPT expression levels, it was observed that high NAMPT expression correlates with shorter patient survival, a finding that is particularly evident in LGG (Fig. 1A-B). This analysis strongly suggests the importance of NAMPT as a therapeutic target and prompted us to further investigate the issue. NAMPT expression was then evaluated in patient-derived GSCs, comparing them with normal human astrocytes (NHA) and a commercially available glioblastoma cell line (U251), by different approaches: quantitative RT-PCR for mRNA levels, western blot analysis and immunocytochemistry were performed to assess protein expression and cellular distribution. NAMPT expression was also evaluated in other non-tumor cell types to assess whether the inhibition of NAMPT led to any damage in non-tumor cells as well. Notably, prior to each series of experiments the stem-like nature of glioblastoma stem cells was validated by assessing the expression of Nestin, Sox-2, and N-cadherin (Fig. S1).

3.1.1. RT-qPCR

Quantitative RT-PCR experiments were performed as described in the Methods section, data are expressed by the ΔΔCt method, with NAMPT Ct values found in NHA set as the reference. As shown in Fig. 1 C, GSCs exhibited a striking higher NAMPT mRNA expression compared with both astrocytes and U251 cells. Surprisingly, HUVEC and differentiated neuron-like SH-SY5Y cells (Fig. S2) were found to display a different NAMPT expression pattern, compared to NHA, more similar to GSCs; results are reported in the supplementary data, Fig. S3. Experiments were performed at least three times in triplicate using different cell preparations.

3.1.2. Western blot

Western blot analyses were then performed to assess whether differences in mRNA expression were mirrored at the protein level. As illustrated in Fig. 1D, NAMPT protein abundance was also significantly higher in GSCs relative to astrocytes and U251 cells. An interesting aspect highlighted by these data is that U251, a GBM cell line commonly used in the literature, displays a NAMPT expression pattern significatively different from GSCs, showing that the two cell models are not equivalent and can therefore lead to different results and conclusions regarding the response to NAMPT inhibitors.

3.1.3. Immunocytochemistry

Finally, immunocytochemistry performed by confocal microscopy confirmed the differential expression of NAMPT between NHA and GSCs (Fig. 1E). NAMPT appeared to be mainly diffused in the cytoplasm in all the cell lines.

3.1.4. ELISA assays

While intracellular NAMPT acts primarily as a metabolic enzyme, a fraction of this protein is released into the extracellular medium, eNAMPT, and functions predominantly as a potent cytokine-like signaling molecule within the tumor microenvironment. To evaluate if eNAMPT was actually released by GSCs, an ELISA test was performed on the cell medium, but no significant release was found (Fig. S4), supporting the hypothesis that the NAMPT enzyme is mainly employed

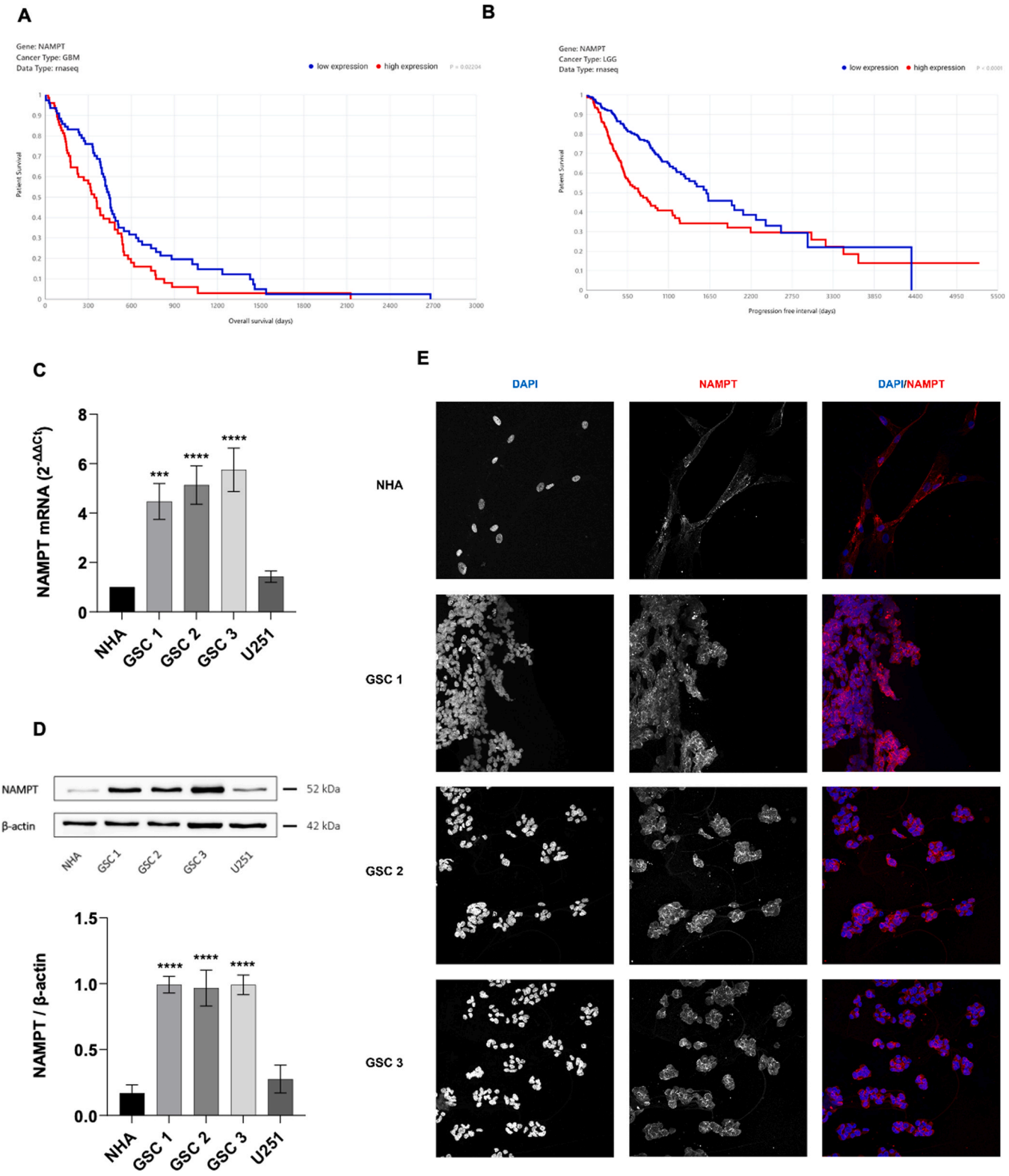

Fig. 1. XXX.

intracellularly by GSCs for NAD + synthesis.

3.2. *NAMPT inhibitors strongly affect GSC survival*

To elucidate the role of NAMPT in GSCs growth and survival, we investigated the functional consequences of NAMPT inhibition by cell viability assays, performed using increasing concentrations of NAMPT inhibitors and the MTS assay, as described in the Methods section. Three molecules were tested: the commercially available FK866 and two other molecules structurally related to FK866 named MV78 and MV87 [18], synthesized by the medicinal chemistry group at the University of Novara. Based on previous reports [20,21] and preliminary experiments, concentrations ranging from 1 nM to 1 μM (1 nM, 5 nM, 10 nM, 100 nM, 1 μM) were tested in a 48 h exposure. The three GSC lines were

analyzed, together with the commercially available human glioblastoma cell line U251 and NHA. As shown in Fig. 2 A, D, the already known NAMPT inhibitor FK866 induced a pronounced reduction in GSC viability already at 1 nM, whereas U251 cells and astrocytes were unaffected. A decrease in U251 cell viability was observed only at 100 nM, while astrocytes did not display sensitivity to FK866 at any tested concentration. Analogous experiments were performed using the other two NAMPT inhibitors, MV78 and MV87: both compounds reduced GSC viability at concentrations of 5–10 nM (Fig. 2B, C, E, F). Notably, in line with the results obtained with FK866, NHA remained insensitive to NAMPT inhibition, even at the highest concentration tested (1 μM). When employing HUVECs and differentiated neuron-like SH-SY5Y as a non-malignant cell control, no cell toxicity was detectable for HUVEC at all tested concentrations (Figure S5, A-C), whereas for differentiated SH-SY5Y cells a partial reduction of viability was detected for concentrations $\geq$ 5 nM for FK866 or 10 nM for MV78 and MV87 (Fig. S5, D-F). Based on these findings, time-course analyses were performed at 5 nM to evaluate the kinetics of the response. As illustrated in Fig. 3A-C, a marked reduction in cell viability was already evident after 48 h of treatment. Consequently, this exposure time was set for all the following experiments. All data were derived from four independent experiments, each conducted in quadruplicate. Based on these data, IC_{50} values were calculated for each compound and each cell line (Table 1).

To further elucidate the correlation between NAMPT expression (NAMPT/β-actin ratio via WB) and GSC survival (% of control, MTS) a correlation analysis was performed by using GraphPad Prism: the results in Fig. 3D-F show a strong and significant correlation between NAMPT expression and sensitivity to inhibitors in the cells evaluated, confirming the hypothesis that NAMPT could be a GSC-specific target that spares non-tumor cells from toxicity at the investigated doses. In addition, as a functional correlate, we measured NADH produced by NHA, GSCs and U251 and results mirror the data previously shown (Fig. 4 A).

3.3. GSCs lack NAPRT expression compared to GBM and astrocytes

NAMPT is the rate-limiting enzyme in the NAD + salvage pathway, while NAPRT, nicotinate (NA) phosphoribosyltransferase, is the rate-limiting enzyme in NAD + synthesis; the two enzymes use different substates for NAD + synthesis (NAM, nicotinamide, and NA) and represent parallel metabolic pathways that contribute to maintain cellular NAD + pools. Non-tumor cells can utilize both pathways while in many human cancers, including gliomas (particularly those with IDH mutations) [22], the NAPRT gene is frequently silenced, making cancer cells entirely dependent on NAMPT for their survival. To evaluate whether this expression pattern was also characteristic of GSCs, as well as any potential differences compared to NHA, U251, and other non-tumor cells, NAPRT expression was assessed using qRT-PCR. Fig. 4B shows that NAPRT expression is significantly lower in GSCs compared to NHA (***$p < 0.001$ and ****$p < 0.0001$ vs NHA). An opposite trend was observed for HUVEC, which displayed a significantly higher NAPRT expression as compared to NHA (Fig. S6). Differentiated SH-SY5Y cells display a low NAPRT expression, compared to NHA, but, despite this, they are still less sensitive to NAMPT inhibitors than GSCs (Fig. S5). Overall, this pattern accounts for the high selectivity of NAMPT inhibitors towards GSCs, which rely almost exclusively on the NAMPT-dependent pathway.

3.4. Treatment with NAMPT inhibitors triggered partial autophagy and apoptosis in GSCs

We investigated the mechanism by which NAMPT inhibitors induce cell death in GSCs by distinct approaches. Since in the literature autophagy, senescence and apoptotic cell death are reported in cancer cells following NAMPT inhibitors treatment [20,21,23–25], we tested all these pathways in our cell model.

3.4.1. Apoptosis pathway

Cells were exposed to the two most effective inhibitors under the experimental conditions described above (5 nM, 48 h) and subjected to FACS analysis; after treatments, NHA and GSCs were scraped, rinsed in PBS and incubated with Annexin/PI, as described in the Methods section. Cytofluorimetric analysis showed that NHA cells remained highly viable after 48 h of treatment, with no evidence of apoptosis or necrosis. In contrast, GSC 1 displayed a significant reduction in viability compared with untreated controls. FK866 treatment showed a greater tendency to induce apoptosis, whereas MV78-treated cells exhibited a higher proportion of necrotic cells. However, the distribution of apoptotic and necrotic cell populations did not differ significantly between the two treatments (Fig. 5 A). To further confirm these data, under the same conditions, the cell extracts were subjected to western blot analysis to detect caspase 8. Results are shown in Fig. 5B, the active caspase 8 was detected in all the three GSC lines while NHA showed no active caspase-8 after treatment with FK866.

3.4.2. Autophagy pathway

NAD + depletion can trigger stress responses, including autophagy, which is sometimes interpreted as an adaptive attempt and other times as part of an autophagy-associated type of cell death [23,24,26]. However, the issue is still largely unclear: in some models, autophagy is increased and protective, whereas in others NAMPT inhibition leads to energy collapse accompanied by apoptotic/necrotic death, without a clear lethal autophagic component [6,20,21]. In GSCs no data are available about NAMPT inhibitors induced autophagy, therefore we decided to address the issue. In detail, the same protocol described above was applied to detect active beclin1 and LC3 proteins, active beclin1 was detected by western blot analysis in all cell lines (Fig. 6 A), while active LC3 was only detected when GSCs were treated with the FK866 inhibitor (Fig. 6B), while no signal appeared after treatment with MV78.

This apparent discrepancy could suggest a weaker effect of MV78 compared to FK866. These data, however, do not rule out the possibility that NAD + depletion could induce autophagy in GSCs and seem to suggest that several mechanisms and pathways play a role in triggering cell death.

3.4.3. Senescence

Finally, the senescence pathway was investigated by the β-Galactosidase test, as described in the methods section. Under the experimental conditions described above, only a slight β-Galactosidase increase was detected in the presence of the inhibitors (Fig. 6 C). Taken together, these results suggest that both FK866 and MV78 inhibitors induce cell death in GSCs mainly due to apoptosis pathway activation, even though complex and overlapping mechanisms acting concomitantly cannot be excluded.

3.5. siRNA-mediated NAMPT silencing leads to cell death in GSCs

To determine if the response to NAMPT inhibitors resulted solely from enzyme inhibition and to exclude off-target toxicity, we performed NAMPT knockdown experiments in GSCs using specific siRNAs. Additionally, the experiment sought to investigate if NAMPT knockdown in GSCs could replicate the drastic effect observed with the inhibitors. siRNAs were designed as described in the methods section and GSCs were treated 24 h after plating. After further 24 h, FK866 (5 nM, 48 h) was applied to untreated cells in order to evaluate the comparative impact of NAMPT pharmacological inhibition and siRNA silencing. At the end of the incubation period, the cells were subjected to MTS cell viability tests and, in parallel experiments, to western blot analysis. Results are shown in Fig. 7: NAMPT RNA was significantly reduced after 96 h contact with siRNA (Fig. 7 A) and, under the same conditions, also the NAMPT protein levels were significantly reduced (Fig. 7B). In parallel, GSCs treated with siRNA showed a decreased survival ability

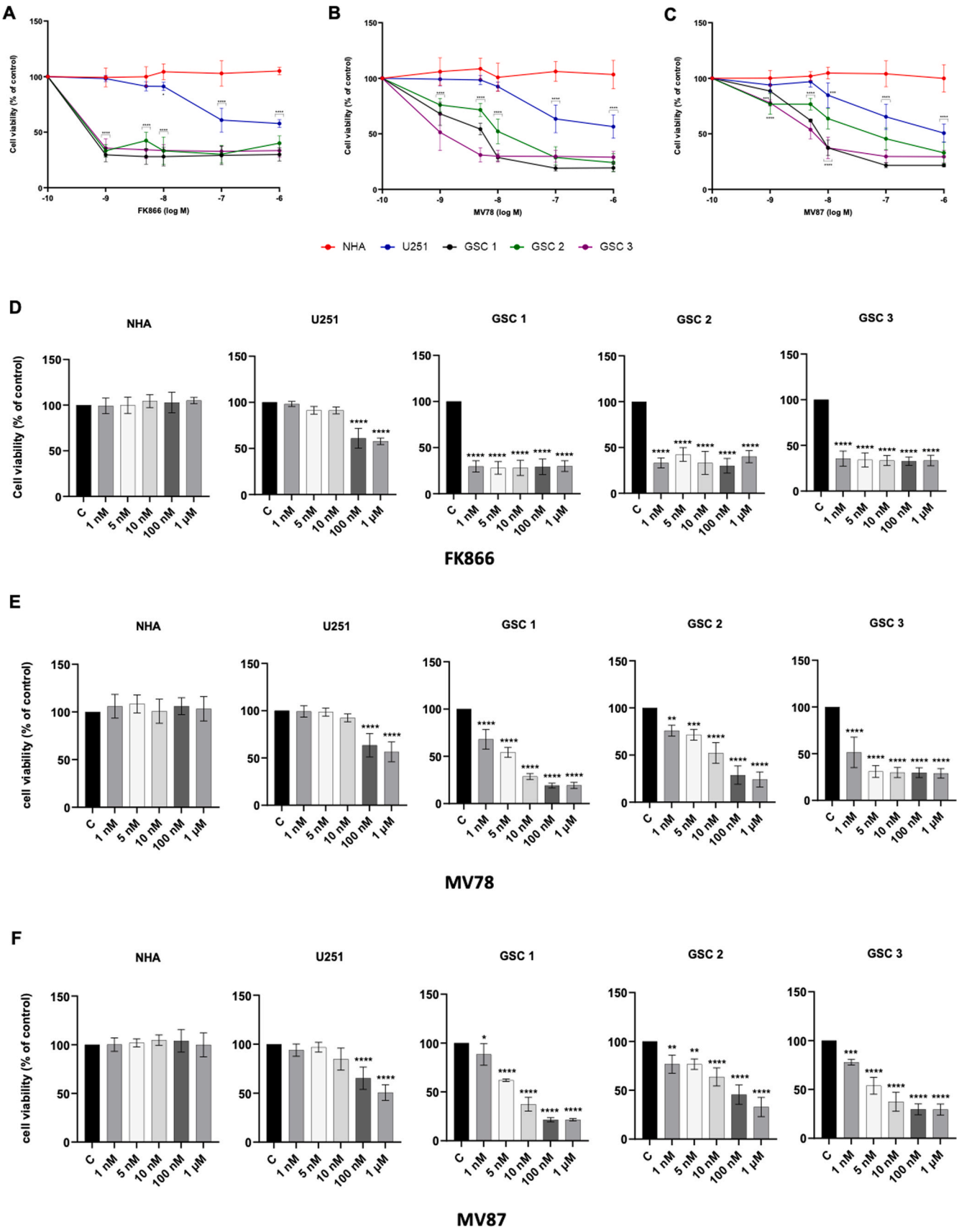
A
B
C
Cell viability (% of control)
FK866 (log M)
MV78 (log M)
MV87 (log M)
NHA
U251
GSC 1
GSC 2
GSC 3
D
E
F
cell viability (% of control)
C
1 nM
5 nM
10 nM
100 nM
1 μM
FK866
MV78
MV87

Fig. 2. XXX.

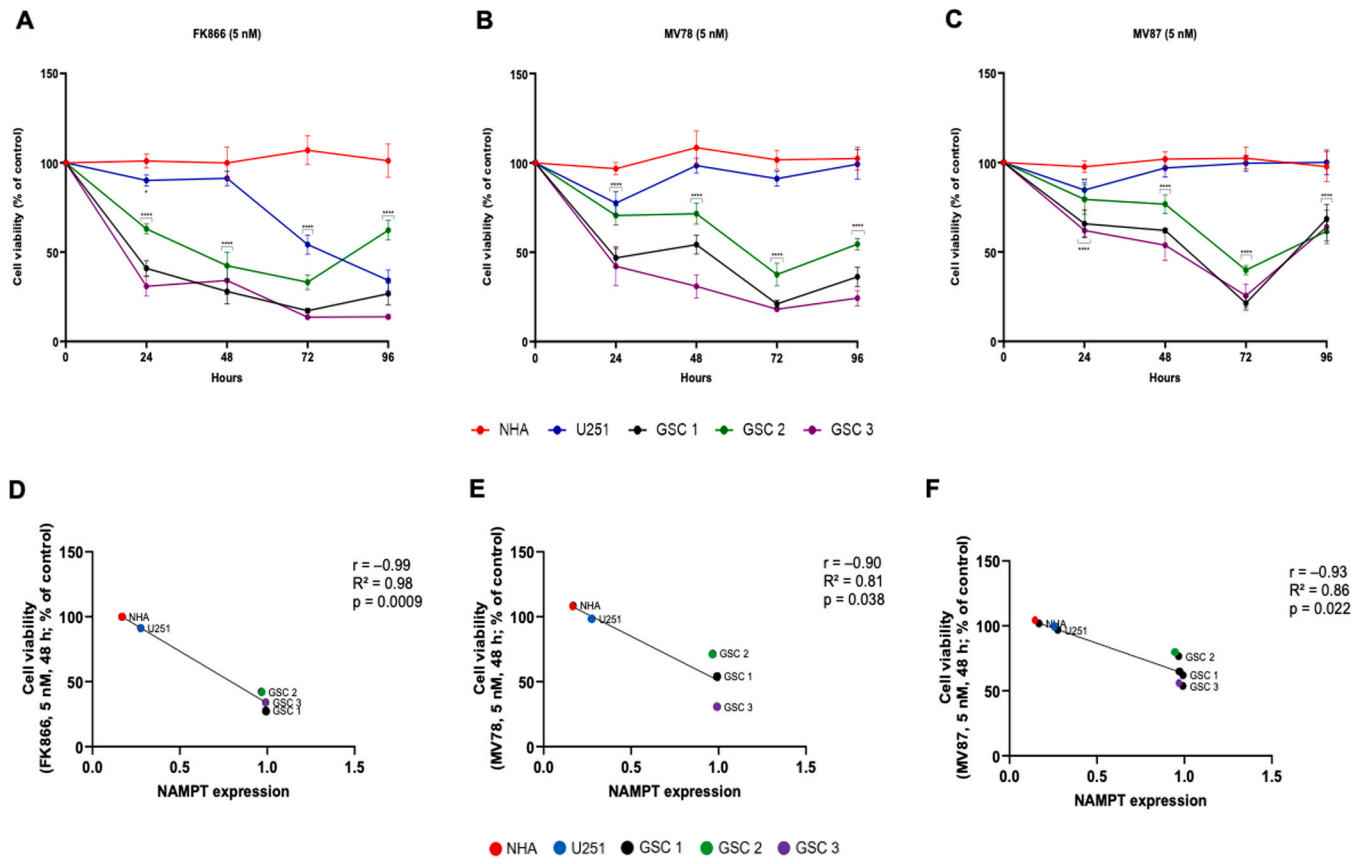

Fig. 3. XXX.

Table 1
Half-maximal inhibitory concentration values of NAMPT inhibitors (IC_{50}). The table reports IC_{50} values calculated by nonlinear regression analysis using GraphPad Prism version 11.

Cell line	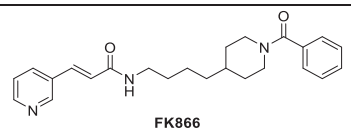 FK866 IC_{50}	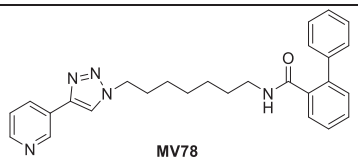 MV78 IC_{50}	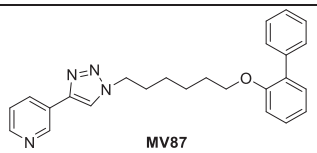 MV87 IC_{50}
GSC 1	872 pM	4.32 nM	10.23 nM
GSC 2	471 pM	20.9 nM	78.41 nM
GSC 3	719 pM	1.54 nM	10.33 nM
U251	1.93 μM	2.90 μM	1.69 μM

compared to untreated control cells under identical experimental conditions (Fig. 7 C). These data confirm the primary role of NAMPT in GSC survival and indicate NAMPT as a strong candidate to selectively target GSCs.

4. Discussion

Current therapies used in GBM target the tumor mass as a whole and, even when it can be reduced either surgically or through pharmacological means or radiation, it is impossible to eradicate GSCs. This results in an increased percentage of therapy-resistant GSCs and leads to disease relapses that are, in fact, untreatable [27]. The aim of this work was, therefore, to verify whether it is possible to selectively target GSCs without destroying healthy cells, and to lay the groundwork for a new use of NAMPT inhibitors, which is more effective and selective against those cells that are difficult to target with other therapeutic means. Nicotinamide phosphoribosyltransferase (NAMPT) plays a rate-limiting and strategic role in tumor metabolism, serving as a key enzyme in the salvage pathway for NAD + biosynthesis. Cancer stem cells, in general, are highly dependent on NAD + synthesis due to their high replicative and metabolic activity (ATP synthesis), to support PARP activity in DNA repair, and sirtuin-dependent oncogenic signaling. Sirtuins

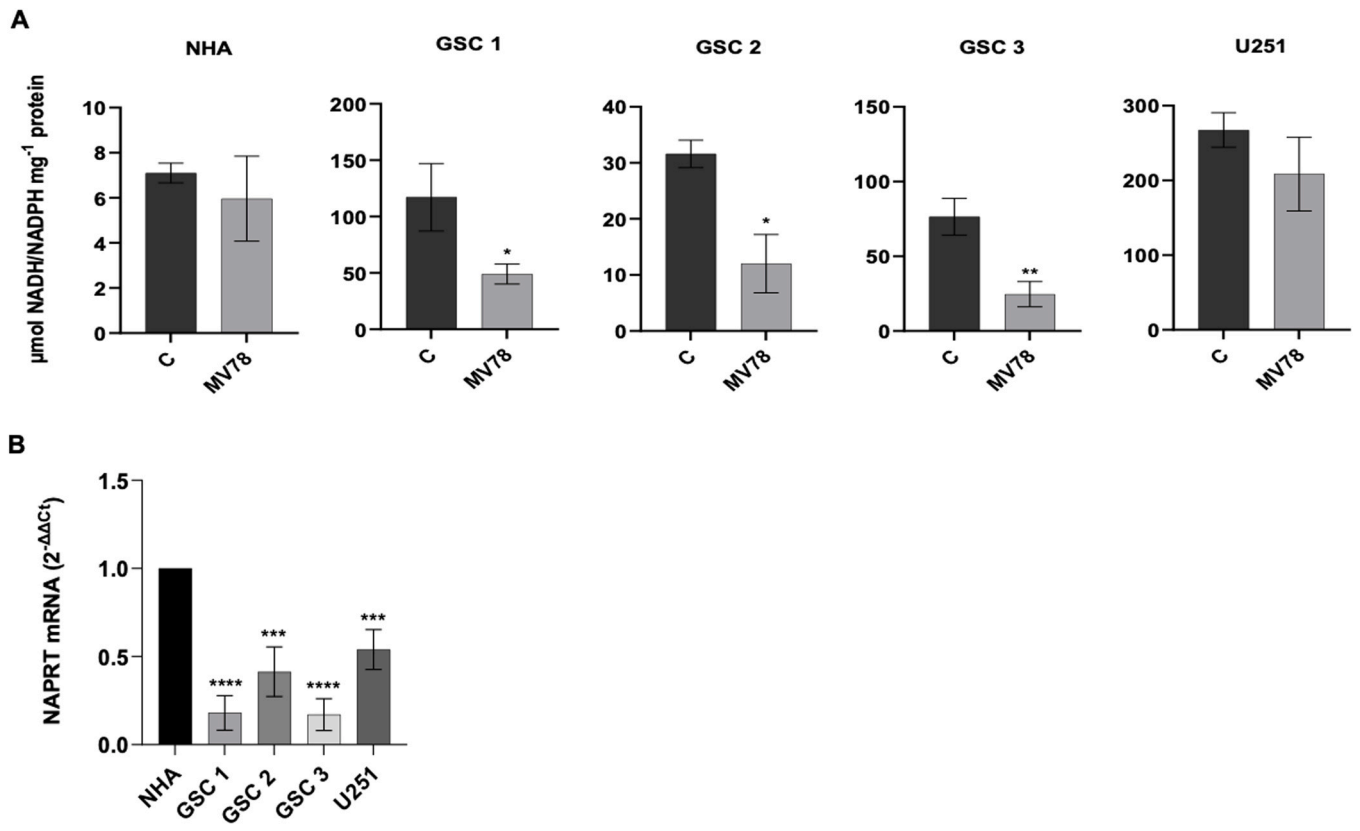

Fig. 4. XXX.

(SIRT1-SIRT7) are a family of epigenetic deacetylase and epilase enzymes. Unlike other deacetylases, sirtuins are strictly dependent on NAD + and, in the deacetylation mechanism, they utilize NAD + , releasing nicotinamide (NAM) as a reaction byproduct. NAM, in turn, is a potent inhibitor of the sirtuins themselves, inhibiting their activity according to a negative feedback loop. NAMPT utilizes the nicotinamide produced by sirtuins and converts it back into nicotinamide mononucleotide (NMN), a precursor of NAD + . It has been shown that in GSCs this loop is used almost exclusively to ensure tumor cell survival [11].

This metabolic framework renders GSCs particularly vulnerable, as they exploit the NAMPT/NAD + axis not only for energetic purposes, but also to maintain their self-renewal program active through the transcriptional regulation of key factors such as SOX2, which, in our model as well, is enormously upregulated (fig. S1). Consequently, the targeted inhibition of NAMPT represents an extremely selective metabolic vulnerability point, as demonstrated by our PCR and western blot data.

While intracellular NAMPT acts primarily as a metabolic enzyme, a fraction of this protein is released into the extracellular medium, eNAMPT, and functions predominantly as a potent cytokine-like signaling molecule within the tumor microenvironment. Secreted by both tumor cells and surrounding stromal or immune cells under stress conditions such as hypoxia and inflammation, eNAMPT binds to specific surface receptors, most notably Toll-like Receptor 4 (TLR4). This interaction triggers a robust intracellular cascade involving the NF-κB, STAT3, and AKT pathways, which actively promotes tumor cell proliferation, angiogenesis, and resistance to apoptosis. To evaluate if eNAMPT was actually released by GSCs, an ELISA test was performed on the cell medium, but no significant release was found (fig. S4), supporting the hypothesis that the NAMPT enzyme is mainly employed intracellularly by GSCs for NAD + synthesis.

The NAMPT inhibitor we used in this study, FK866, was previously used in preclinical studies in neuroblastoma, pancreatic carcinoma, anaplastic meningioma, and murine renal cell carcinoma [28–31] with encouraging results but failed in phase I clinical trial in advanced solid tumors. In that trial, involving 24 patients with refractory solid malignancies, FK866 was administered as a continuous infusion for 96 h every 28 days; the dose-limiting toxicity turned out to be thrombocytopenia, and no objective responses were observed, although 4 patients experienced stable disease for at least 3 months [32]. Therefore, also in light of significant systemic toxicity, this small molecule was discarded. The other two molecules, MV78 and MV87, were synthesized by the Medicinal Chemistry group at the University of Novara starting from the structure of FK866, in an attempt to moderate the systemic toxicity profile of FK866 [18]. Originally, therefore, all these molecules were conceived and also widely used in preclinical studies, for systemic use in solid tumors, including in combination with standard chemotherapeutic agents [28]. Our cell viability data also show that, at active concentrations on GSCs, the inhibitors, particularly FK866 and MV78, have a reduced effect on U251 and no cytotoxic effect on other non-tumor cell populations such as NHA and HUVEC. These data are further supported by the fact that NAMPT silencing closely reproduces the effect of the inhibitors, thereby ruling out off-target effects associated with non-specific toxicity. Interestingly, neuron-like differentiated SH-SY5Y cells displayed a slight cytotoxicity upon treatment with NAMPT inhibitors, although this effect was observed at higher concentrations than the ones effective on GSCs. This result could be explained by comparing the expression levels of NAMPT and NAPRT in these cells: while NAMPT mRNA levels in SH-SY5Y are higher than NHA and similar to HUVEC, NAPRT mRNA levels are similar to NHA, suggesting that neuron cells can also use de NAPRT pathway; however, a slight sensitivity to NAMPT inhibitors cannot be excluded and further experiments on primary neuronal cultures and in vivo, in GBM animal models, will be crucial to clarify this aspect.

The interesting finding emerging from our data is that NAMPT

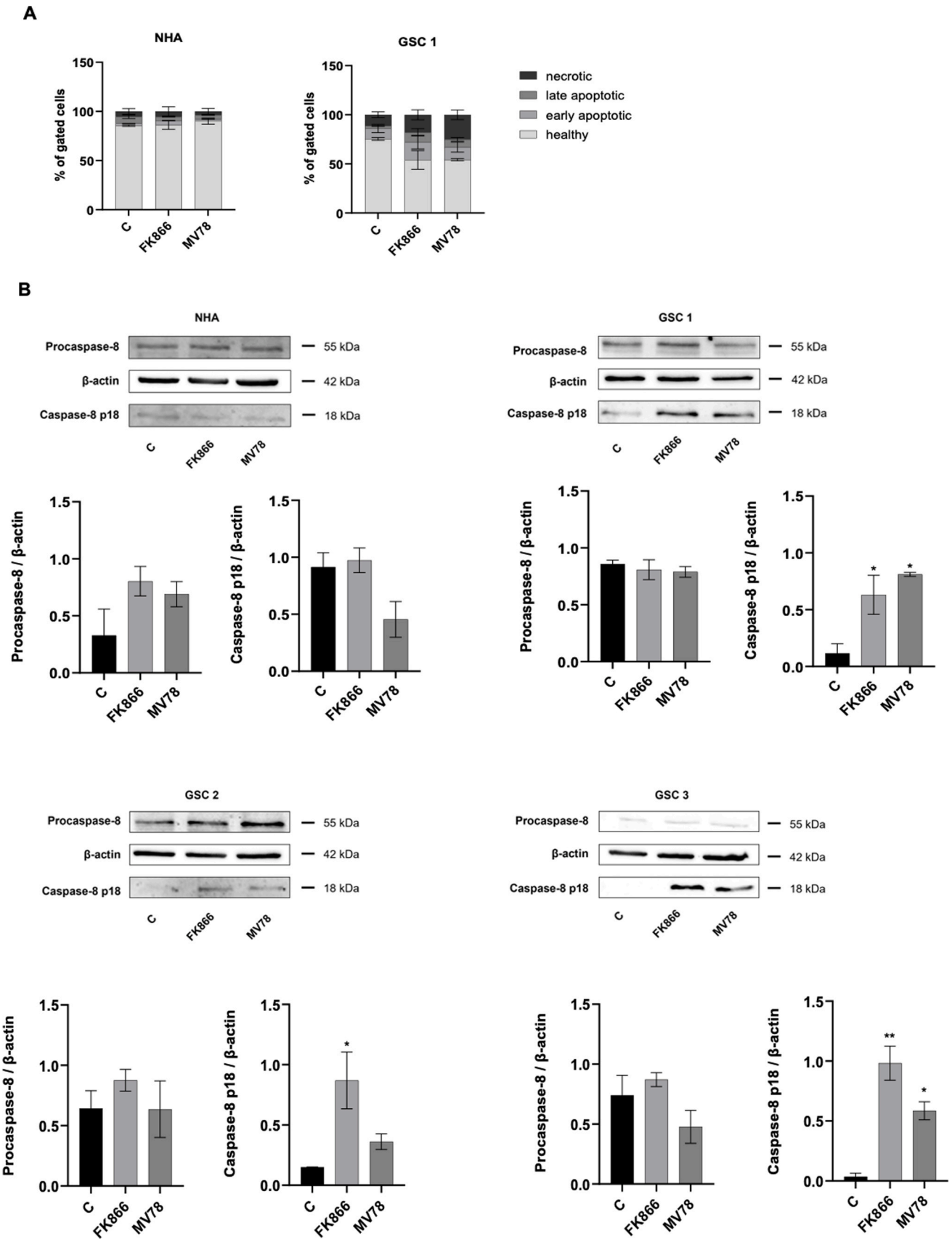
A
NHA
GSC 1
% of gated cells
150
100
50
0
C
FK866
MV78
necrotic
late apoptotic
early apoptotic
healthy
B
NHA
GSC 1
Procaspase-8
β-actin
Caspase-8 p18
55 kDa
42 kDa
18 kDa
Procaspase-8 / β-actin
Caspase-8 p18 / β-actin
1.5
1.0
0.5
0.0
*
GSC 2
GSC 3
**

Fig. 5. XXX.

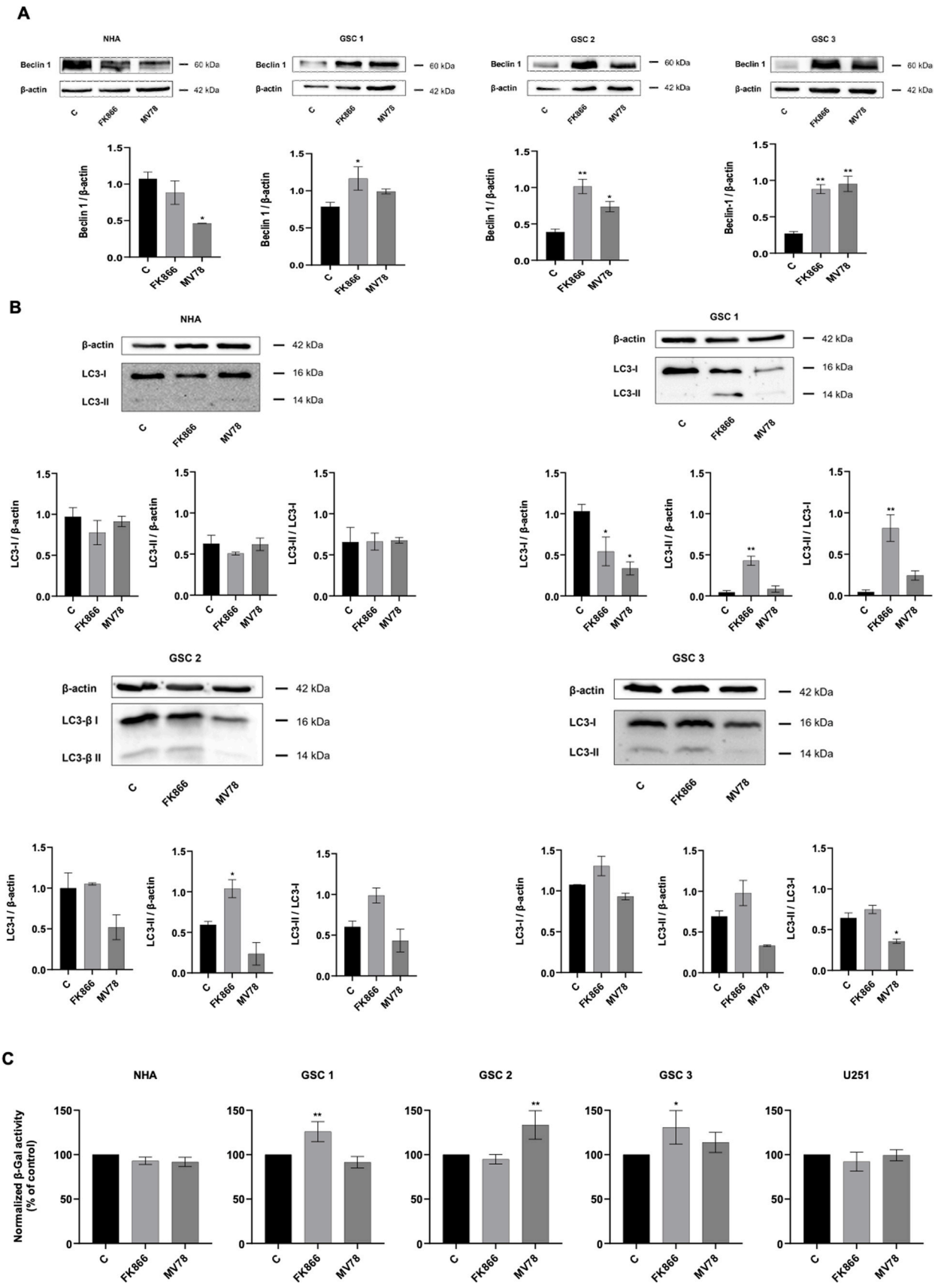
A
NHA
GSC 1
GSC 2
GSC 3
Beclin 1
β-actin
60 kDa
42 kDa
C
FK866
MV78
Beclin 1 / β-actin
Beclin-1 / β-actin
B
LC3-I
LC3-II
LC3-β I
LC3-β II
16 kDa
14 kDa
LC3-I / β-actin
LC3-II / β-actin
LC3-II / LC3-I
C
Normalized β-Gal activity (% of control)
U251

Fig. 6. XXX.

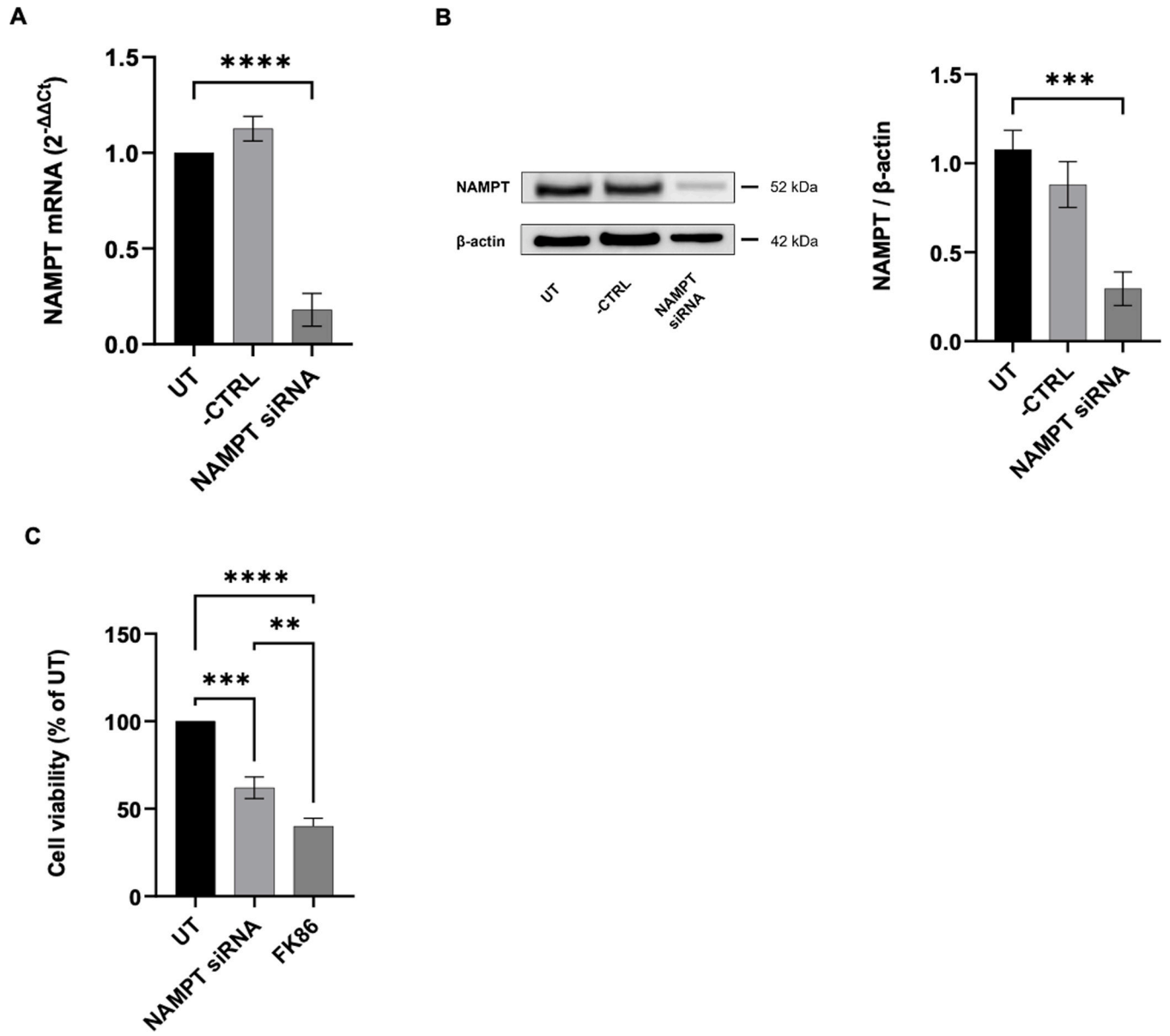

Fig. 7. XXX.

inhibitors alone are capable of inducing cell death in glioma stem cells at very low concentrations, without the need for synergy with other cytotoxic molecules. On the contrary, this does not occur either for non-tumor cells such as NHA, HUVEC, neuron-like differentiated SH5Y or for differentiated tumor cells (such as the U251 cell line). This aspect is very important for understanding the difference in the potential use of NAMPT inhibitors; indeed, previous studies have shown that NAMPT expression is upregulated in GBM and is inversely correlated with the overall survival of patients [10,12,33]. In the literature, it has been observed that a very high percentage of GBM exhibits epigenetic silencing or homozygous deletion of the NAPRT gene, the enzyme that regulates the alternative pathway of NAD + synthesis from nicotinic acid [9,34]. However, these studies were largely conducted on bioptic specimens or tumor cell lines, and the use of NAMPT inhibitors was tested in combination with standard chemotherapy, with less than brilliant results. Given the exceptional sensitivity of GSCs to these inhibitors and, conversely, the scarce or null sensitivity of the other cell types examined in our study, it is possible to hypothesize a use of these inhibitors restricted either to the initial stages of tumor progression or following surgical resection and/or chemo- and radiotherapy treatments. In this way, in fact, it would be possible to selectively target the most sensitive cell population, which is simultaneously the most difficult to eradicate with standard therapies.

We then investigated the mechanisms through which the two most effective inhibitors (FK866 and MV78) induce death in GSCs; our data indicate that the prevalent mechanism is represented by apoptosis, although the concomitant initiation of other pathways, such as autophagy, cannot be ruled out. Furthermore, further studies are necessary to thoroughly investigate the role of SIRT1 and SIRT2 in apoptosis onset induced by NAMPT inhibitors.

In conclusion, in this work we have demonstrated the exceptional cellular selectivity of the inhibitors used: the vast majority of studies in the literature test inhibitors on stabilized and differentiated tumor cell lines (such as U251). This study demonstrates that patient-derived glioma stem cells are extremely more sensitive to the inhibitors compared to the commercial line U251. The IC_{50} values for FK866, MV78, and MV87 drop to picomolar or low nanomolar levels in GSCs, while healthy cells (NHA) and endothelial cells (HUVEC) remain completely unaffected at doses even 1000 times higher (up to 1 μM), as occurs in differentiated neuron-like SH5Y cells (IC_{50}: FK866, 179.20 nM; MV78,

404.40 nM; MV87, 513.60 nM). This opens up the prospect toward a pharmacological use of molecules with a potentially very wide "therapeutic window".

In addition, the knockdown of NAMPT via siRNA closely mirrors the effect of the inhibitors, demonstrating that this effect is on-target and not due to non-specific toxicity of the chemical compounds. A further implication arises from the fact that NAMPT-directed siRNAs could offer a novel therapeutic strategy, potentially via innovative and non-invasive delivery systems [35,36]. Finally, the identification of a molecule effective at extremely low concentrations (1–5 nM) on GSCs, which are responsible for GBM relapses, paves the way for a post-operative local delivery strategy, with the prospect of being able to reduce failures due to systemic use encountered in the past in the clinic.

Funding

This work was supported by Italian Health Ministry grant F13C22001110001_IMMUNO-HUB Ministry of Health – Health Operational Plan, PSC. Trajectory 4 – Interventions for the creation of Life Sciences Hubs in the Pharmaceutical, Biomedical, and Biotechnology sectors.

Declaration of Competing Interest

Authors have no competing interests and declare they have nothing to declare.

Acknowledgements

The authors would like to thank: Dr. Antonio Daga, IRCCS Azienda Ospedaliera Universitaria San Martino – IST, Genova for providing purified GSCs; Prof. Marco Terreni, Department of Drug Sciences at the University of Pavia, for conceiving the IMMUNO-HUB project; Professor Marco Racchi Department of Drug Sciences at the University of Pavia, for his constructive feedback; Professor Sergio Schinelli, who passed away prematurely, for his valuable contribution in the initial phases of the work.

Appendix A. Supporting information

Supplementary data associated with this article can be found in the online version at doi:10.1016/j.biopha.2026.120050.

Appendix B. Supporting information

Supplementary data associated with this article can be found in the online version at doi:10.1016/j.biopha.2026.120050.

Data availability

Data will be made available on request.

References

[1] M. Khabibov, A. Garifullin, Y. Boumber, et al., Signaling pathways and therapeutic approaches in glioblastoma multiforme (Review), Int. J. Oncol. 60 (6) (2022) 69, https://doi.org/10.3892/ijo.2022.5359.
[2] J. Li, L. Feng, Y. Lu, Glioblastoma multiforme: diagnosis, treatment, and invasion, J. Biomed. Res. 37 (1) (2023) 47, https://doi.org/10.7555/JBR.36.20220156.
[3] Q.T. Ostrom, N. Patil, G. Cioffi, K. Waite, C. Kruchko, J.S. Barnholtz-Sloan, CBTRUS statistical report: primary brain and other central nervous system tumors diagnosed in the United States in 2013–2017, Neuro Oncol. 22 (ement_1) (2020) iv1–iv96, https://doi.org/10.1093/neuonc/noaa200.
[4] H. Lee, B. Kim, J. Park, et al., Cancer stem cells: landscape, challenges and emerging therapeutic innovations, Signal. Transduct. Target. Ther. 10 (1) (2025) 248, https://doi.org/10.1038/s41392-025-02360-2.
[5] Y. Wei, H. Xiang, W. Zhang, Review of various NAMPT inhibitors for the treatment of cancer, Front. Pharmacol. 13 (2022), https://doi.org/10.3389/fphar.2022.970553.
[6] W. Zhang, H. Ren, W. Chen, et al., Nicotinamide phosphoribosyltransferase in NAD + metabolism: physiological and pathophysiological implications, Cell. Death Discov. 11 (1) (2025) 371, https://doi.org/10.1038/s41420-025-02672-w.
[7] U. Galli, C. Travelli, A. Massarotti, et al., Medicinal chemistry of nicotinamide phosphoribosyltransferase (NAMPT) inhibitors, J. Med. Chem. 56 (16) (2013) 6279–6296, https://doi.org/10.1021/jm4001049.
[8] M. Kim, H. Kim, B.G. Kang, et al., Discovery of a novel NAMPT inhibitor that selectively targets NAPRT-deficient EMT-subtype cancer cells and alleviates chemotherapy-induced peripheral neuropathy, Theranostics 13 (14) (2023) 5075–5098, https://doi.org/10.7150/thno.85356.
[9] J. Cole, M.C. Guiot, M. Gravel, C. Bernier, G.C. Shore, A. Roulston, Novel NAPRT specific antibody identifies small cell lung cancer and neuronal cancers as promising clinical indications for a NAMPT inhibitor/niacin co-administration strategy, Oncotarget 8 (44) (2017) 77846–77859, https://doi.org/10.18632/oncotarget.20840.
[10] A.D. Gujar, S. Le, D.D. Mao, et al., An NAD $^{+}$ -dependent transcriptional program governs self-renewal and radiation resistance in glioblastoma, Proc. Natl. Acad. Sci. 113 (51) (2016), https://doi.org/10.1073/pnas.1610921114.
[11] A. Lucena-Cacace, M. Umeda, L.E. Navas, A. Carnero, NAMPT as a dedifferentiation-inducer gene: NAD+ as core axis for glioma cancer stem-like cells maintenance, Front. Oncol. 9 (2019), https://doi.org/10.3389/fonc.2019.00292.
[12] A. Lucena-Cacace, D. Otero-Albiol, M.P. Jiménez-García, J. Peinado-Serrano, A. Carnero, NAMPT overexpression induces cancer stemness and defines a novel tumor signature for glioma prognosis, Oncotarget 8 (59) (2017) 99514–99530, https://doi.org/10.18632/oncotarget.20577.
[13] H. Tang, L. Wang, T. Wang, et al., Recent advances of targeting nicotinamide phosphoribosyltransferase (NAMPT) for cancer drug discovery, Eur. J. Med. Chem. 258 (2023) 115607, https://doi.org/10.1016/j.ejmech.2023.115607.
[14] C.M. Heske, Beyond energy metabolism: exploiting the additional roles of NAMPT for cancer therapy, Front. Oncol. 9 (2020), https://doi.org/10.3389/fonc.2019.01514.
[15] M. Paolillo, M. Galiazzo, A. Daga, et al., An RGD small-molecule integrin antagonist induces detachment-mediated anoikis in glioma cancer stem cells, Published online October 3,, Int. J. Oncol. (2018), https://doi.org/10.3892/ijo.2018.4583.
[16] J. Kovalevich, D. Langford, 2013, Consid. Use SH-SY5Y Neuroblastoma Cells Neurobiol.92110.1007/978-1-62703-640-5_2.
[17] M.M. Shipley, C.A. Mangold, M.L. Szpara, Differentiation of the SH-SY5Y Human Neuroblastoma Cell Line, J. Vis. Exp. (108) (2016), https://doi.org/10.3791/53193.
[18] C. Travelli, S. Aprile, R. Rahimian, et al., Identification of novel triazole-based nicotinamide phosphoribosyltransferase (NAMPT) inhibitors endowed with antiproliferative and antiinflammatory activity, J. Med. Chem. 60 (5) (2017) 1768–1792, https://doi.org/10.1021/acs.jmedchem.6b01392.
[19] K.J. Livak, T.D. Schmittgen, Analysis of relative gene expression data using real-time quantitative PCR and the 2−ΔΔCT method, Methods 25 (4) (2001) 402–408, https://doi.org/10.1006/meth.2001.1262.
[20] M. Hasmann, I. Schemainda, FK866, a highly specific noncompetitive inhibitor of nicotinamide phosphoribosyltransferase, represents a novel mechanism for induction of tumor cell apoptosis, Cancer Res. 63 (21) (2003) 7436–7442.
[21] P. Sharma, J. Xu, K. Williams, et al., Inhibition of nicotinamide phosphoribosyltransferase (NAMPT), the rate-limiting enzyme of the nicotinamide adenine dinucleotide (NAD) salvage pathway, to target glioma heterogeneity through mitochondrial oxidative stress, Neuro Oncol. 24 (2) (2022) 229–244, https://doi.org/10.1093/neuonc/noab175.
[22] K. Tateishi, H. Wakimoto, A.J. Iafrate, et al., Extreme vulnerability of IDH1 mutant cancers to NAD+ depletion, Cancer Cell. 28 (6) (2015) 773–784, https://doi.org/10.1016/j.ccell.2015.11.006.
[23] R.A. Billington, A.A. Genazzani, C. Travelli, F. Condorelli, NAD depletion by FK866 induces autophagy, Autophagy 4 (3) (2008) 385–387, https://doi.org/10.4161/auto.5635.
[24] M. Cea, A. Cagnetta, M. Fulciniti, et al., Targeting NAD+ salvage pathway induces autophagy in multiple myeloma cells via mTORC1 and extracellular signal-regulated kinase (ERK1/2) inhibition, Blood 120 (17) (2012) 3519–3529, https://doi.org/10.1182/blood-2012-03-416776.
[25] T. Nacarelli, T. Fukumoto, J.A. Zundell, et al., NAMPT inhibition suppresses cancer stem-like cells associated with therapy-induced senescence in ovarian cancer, Cancer Res. 80 (4) (2020) 890–900, https://doi.org/10.1158/0008-5472.CAN-19-2830.
[26] M.A. Rahman, M. Jalouli, M. Al-Zharani, E. Hoque Apu, A.H. Harrath, Mechanistic insights into autophagy-dependent cell death (ADCD): a novel avenue for cancer therapy, Cells 14 (14) (2025) 1072, https://doi.org/10.3390/cells14141072.
[27] F. Eckerdt, L.C. Platanias, Emerging role of glioma stem cells in mechanisms of therapy resistance, Cancers (Basel) 15 (13) (2023) 3458, https://doi.org/10.3390/cancers15133458.
[28] C. Travelli, V. Drago, E. Maldi, et al., Reciprocal potentiation of the antitumoral activities of FK866, an inhibitor of nicotinamide phosphoribosyltransferase, and etoposide or cisplatin in neuroblastoma cells, J. Pharmacol. Exp. Ther. 338 (3) (2011) 829–840, https://doi.org/10.1124/jpet.111.184630.
[29] C.C.S. Chini, A.M.G. Guerrico, V. Nin, et al., Targeting of NAD metabolism in pancreatic cancer cells: potential novel therapy for pancreatic tumors, Clin. Cancer Res. 20 (1) (2014) 120–130, https://doi.org/10.1158/1078-0432.CCR-13-0150.
[30] Y. Deng, B. Hu, Y. Miao, et al., A nicotinamide phosphoribosyltransferase inhibitor, fk866, suppresses the growth of anaplastic meningiomas and inhibits immune checkpoint expression by regulating STAT1, Front. Oncol. 12 (2022), https://doi.org/10.3389/fonc.2022.836257.

[31] J. Drevs, R. Löser, B. Rattel, N. Esser, Antiangiogenic potency of FK866/K22.175, a new inhibitor of intracellular NAD biosynthesis, in murine renal cell carcinoma, Anticancer. Res. 23 (6C) (2003) 4853–4858.
[32] K. Holen, L.B. Saltz, E. Hollywood, K. Burk, A.R. Hanauske, The pharmacokinetics, toxicities, and biologic effects of FK866, a nicotinamide adenine dinucleotide biosynthesis inhibitor, Invest. New. Drugs 26 (1) (2008) 45–51, https://doi.org/10.1007/s10637-007-9083-2.
[33] Q. Guo, N. Han, L. Shi, et al., NAMPT: a potential prognostic and therapeutic biomarker in patients with glioblastoma, Published online July 10, Oncol. Rep. (2019), https://doi.org/10.3892/or.2019.7227. Published online July 10.
[34] M. Watson, A. Roulston, L. Bélec, et al., The small molecule GMX1778 Is a potent inhibitor of NAD^+ biosynthesis: strategy for enhanced therapy in nicotinic acid phosphoribosyltransferase 1-deficient tumors, Mol. Cell. Biol. 29 (21) (2009) 5872–5888, https://doi.org/10.1128/MCB.00112-09.
[35] M. Serra, A. Buccellini, M. Paolillo, Knocking on cells' door: strategic approaches for miRNA and siRNA in anticancer therapy, Int. J. Mol. Sci. 26 (17) (2025 Sep 6) 8703, https://doi.org/10.3390/ijms26178703.
[36] B. Arjmand, A.R. Mojavezi, A. Kamroo, R.K. Yazdi, M. Rezaei-Tavirani, M. S. Vahedi, Advances in intranasal delivery of exosomes for central nervous system disorders, Mol. Neurobiol. 63 (1) (2025 Nov 27) 193, https://doi.org/10.1007/s12035-025-05563-4.